Medical Image Analysis 16 (2012) 227–238

Contents lists available at ScienceDirect

Medical Image Analysis

journal homepage: www.elsevier.com/locate/media

A novel approach for improved tractography and quantitative analysis of probabilistic fibre tracking curves

Nagulan Ratnarajah [a,*], Andrew Simmons [b,c], Oleg Davydov [d], Ali Hojjatoleslami [a]

[a] Medical Image Computing, School of Biosciences, University of Kent, UK
[b] Neuroimaging Department, Institute of Psychiatry, King's College London, UK
[c] NIHR Biomedical Research Centre for Mental Health at the South London and Maudsley NHS Foundation Trust and Institute of Psychiatry, King's College London, UK
[d] Department of Mathematics and Statistics, University of Strathclyde, UK

ARTICLE INFO

Article history:
Received 22 September 2010
Received in revised form 27 May 2011
Accepted 12 July 2011
Available online 10 August 2011

Keywords:
Probabilistic fibre tracking
Average curves
Branching
Quantitative analysis

ABSTRACT

This paper presents a novel approach for improved diffusion tensor fibre tractography, aiming to tackle a number of the limitations of current fibre tracking algorithms, and describes a quantitative analysis tool for probabilistic tracking algorithms. We consider the sampled random paths generated by a probabilistic tractography algorithm from a seed point as a set of curves, and develop a statistical framework for analysing the curve-set geometrically that finds the average curve and dispersion measures of the curve-set statistically. This study is motivated firstly by the goal of developing a robust fibre tracking algorithm, combining the power of both deterministic and probabilistic tracking methods using average curves. These typical curves produce strong connections to every anatomically distinct fibre tract from a seed point and also convey important information about the underlying probability distribution. These single well-defined trajectories overcome a number of the limitations of deterministic and probabilistic approaches. A new clustering algorithm for branching curves is employed to separate fibres into branches before applying the averaging methods. Secondly, a quantitative analysis tool for probabilistic tracking methods is introduced using statistical measures of curve-sets. Results on phantom and *in vivo* data confirm the efficiency and effectiveness of the proposed approach for the tracking algorithm and the quantitative analysis of the probabilistic methods.

1. Introduction

Fibre tractography using diffusion MR images is a promising method for reconstructing the pathways of white matter fasciculi in the human brain. This method allows one to study the anatomical connectivity of the brain and is an essential diagnostic tool for a number of neurological diseases. A variety of algorithms have been proposed aiming to generate fibre-tract trajectories. Generally these algorithms can be categorised into two main types, deterministic and probabilistic. Deterministic approaches (Basser et al., 2000; Mori et al., 1999; Lazar et al., 2003a) are based on the assumption that the principal eigenvector (PEV) of the diffusion tensor is parallel to the underlying dominant fibre direction in each image voxel. They propagate a single pathway bi-directionally from a seed point by moving in a direction that is parallel to the PEV. These approaches are capable of creating anatomically reliable reconstructions of major white matter tracts. However, they do not correctly deal with branching of white matter tracts as such algorithms produce only one path per seed point and there is no measure describing the uncertainty of the reconstructed trajectories.

Probabilistic tractography algorithms (Friman et al., 2006; Hagmann et al., 2003; Jones, 2008; Lazar and Alexander, 2005) have been developed to overcome the shortcomings of deterministic methods. The aim of probabilistic tracking methods is to provide a natural approach for modelling uncertainty and generate multiple curves originating from a seed point. Probabilistic methods have also been developed to attempt to resolve fibre crossings at the intravoxel level under looser constraints, for example in terms of stopping criteria, allowing them to pass through low-anisotropy areas and to penetrate deeper into gray matter (Behrens et al., 2003), and these methods allow branching of white matter tracts. Generally, probabilistic tracking methods have three stages. In the first stage, they model the uncertainty at each voxel using a probability density function (PDF) of fibre orientations. In the second stage, the tracking algorithm repeats a streamline propagation process many times (typically between 100 and 10,000 per seed point) from a seed point with the propagation direction randomly sampled from the PDF of fibre orientations. The connection probability from a seed point to a random voxel within the dataset is defined as the frequency with which streamlines pass through

* Corresponding author.
E-mail address: rn54@kent.ac.uk (N. Ratnarajah).

1361-8415/$ - see front matter © 2011 Elsevier B.V. All rights reserved.
doi:10.1016/j.media.2011.07.005

the voxel, normalised for the total number of repetitions of the streamline propagation process. Finally a global connectivity map is estimated, using the connection probabilities between all the voxels in the image and the seed point.

The deterministic tractography approaches have several advantages over probabilistic tractography for some applications such as neurosurgery. Firstly, visualisation of the deterministic streamline trajectories is similar to the expected *in vivo* white matter fibre tracts; whereas the output of probabilistic methods is a connectivity map, which is not a single well-defined trajectory, but rather a spatial distribution. These connectivity maps contain dense 3D volumes of potential connectivities, which cannot be easily inspected. The determination of a connectivity map is also a time-consuming process and requires large amounts of memory. Connection probability maps derived using frequency of connection methods demonstrate high frequency connections close to the seed point and low frequency connections at distance from the seed point. This can lead to difficulty in interpreting tracking results, because the derived connection probabilities are not comparable at different distances from the seed point (Morris et al., 2008). The connectivity maps from probabilistic tractography are no more than an indication of the number of times that a range of trajectories pass through a voxel from the seed point. The aim of any tractography algorithm is to reconstruct tracts that accurately correlate with the underlying white matter pathways. Given a 3D volume of connectivity maps with a dense map of frequent visitations, it is extremely difficult to identify the most probable trajectory. In short, neurosurgeons are more interested to know where the fibre pathways are located, rather than where they might be probable.

Secondly, output tracts from probabilistic methods can leak into unexpected regions producing incorrect connections of white matter (Descoteaux et al., 2007). These outlier bundles are also considered for the calculation of connection probability and the output map.

In this study, we present an improved tractography algorithm, which combines the advantages of deterministic and probabilistic approaches and overcomes a number of the limitations of such techniques described above. Building on our preliminary studies (Ratnarajah et al., 2009; Ratnarajah et al., 2010a; Ratnarajah et al., 2010b), we consider the fibre pathways of a probabilistic method from a seed point as a set of curves. We then compute a representative skeleton curve to every anatomically distinct region from the seed point directly from the generated curves using branch-clustering and average curves. We define two statistical methods for computing average curves and a dispersions measure of a collection of probabilistic tracking curve-sets.

Clustering of the branching curves is applied before computing the average curves to deal with bimodality in the probabilistic results, i.e. the points at which the results suggest that the tracts are branching into two or more groups from a seed point. Several fibre clustering approaches, which are fully automatic and take advantage of the similarity of the fibre paths, have been proposed (Brun et al., 2004; O'Donnell et al., 2006; Li et al., 2010). These fibre clustering methods analyse a collection of tractographic paths, which are generated from many seed points using deterministic algorithms, and separate them into clusters that contain paths with similar shape and spatial position. In the approach described here we develop a new clustering algorithm for estimating the branch curve-sets of generated probabilistic curves from a seed point. Probabilistic curves generated from a single seed point can branch into two or more main paths. We therefore consider only the spatial positions of the curve points of the collection of curves and separate the branches using a hierarchical distance-based clustering algorithm. Moreover, our algorithm is computationally efficient and allows outlier detection. Branches with few fibres, as well as the shortest and longest fibres within a branch are considered as outliers and are excluded before calculating the average curves in a pre-processing step. This pre-processing step is used to ensure that the branches selected for average measures are strongly connected to cortical regions and outliers are removed. Two different averaging methods are then applied for each set of branched curves to compute representative curves. All of the branch average curves from the seed point are concatenated to produce the final output of the improved tractography.

We evaluate the tracking algorithm quantitatively on a hardware diffusion tensor tractography phantom used for the MICCAI 2009 Fiber Cup which simulates several complex pathway interactions and qualitatively on data acquired *in vivo* from a human brain. To demonstrate the robustness of our algorithm, we compared the resultant tracts with the ground truth in the phantom data. To evaluate *in vivo* data we computed trajectories in two well-defined white matter structures: the corpus callosum and the pyramidal tracts. Three previously published commonly used probabilistic tracking algorithms (a parametric, a non-parametric and a random-walk) are applied to generate numerous possible tracts from each seed point.

Generally, conventional single-tensor fibre tracking approaches have difficulties in brain regions where fibre bundles cross. In such cases, a single diffusion tensor model is no longer valid. The development of new models based on high angular resolution diffusion imaging (HARDI) seeks to provide solutions to this problem (Tuch et al., 2002; Tuch, 2004; Jansons and Alexander, 2003; Wedeen et al., 2008). HARDI-based deterministic tractography and probabilistic tractography methods have recently been published in the literature (Berman et al., 2008; Descoteaux et al., 2009; Kreher et al., 2005; Perrin et al., 2005) and their results have shown successful reconstruction of multiple intravoxel fibres and improved reliability of tractography. Therefore, to improve the robustness of our tractography algorithm for dealing with crossing fibres and to show that the proposed algorithm can be extended to techniques beyond the single-tensor DT model, we applied a two-tensor random-walk method to the *in vivo* data.

There is a strong clinical need for an objective mathematical framework for quantitative analysis of fibre tracking curves. Generally, the mathematical frameworks described in the literature to date (Maddah et al., 2008; Wassermann et al., 2010) have aimed to facilitate subsequent clustering and group-based statistical analysis of fibre bundles. Recently, Wassermann et al. (2010) presented a mathematical framework that facilitates mathematical operations between tracts using an inner product between fibres with the aim of producing an automated clustering method. While analysing fibre tracking curves geometrically is a promising notion, relatively little attention has been paid to this area, with a few exceptions. Some studies have been motivated by the problem of analysing the shapes of fibre tracts (Batchelor et al., 2006; Savadjiev et al., 2006), presenting a geometric framework for studying the shapes of curves in 3D. Other studies have investigated coarse geometrical descriptors of fibre tracts, such as smoothness, curvature, torsion and length (Basser, 1997; Ding et al., 2003). Corouge et al. (2006) proposed a framework for quantitative tract-oriented DTI analysis that includes tensor interpolation and averaging, using nonlinear Riemannian symmetric space. Durrleman et al. (2009) proposed a framework where sets of curves and surfaces are modelled as currents. This framework provides tools for computing statistics such as means and modes of a population of shapes. However, this framework is more generic than ours and the population data comes from different subjects. To our knowledge, this is the first paper to describe a statistical framework for analysing probabilistic fibre tracking curve-sets geometrically.

In this work, we introduce a quantitative analysis tool for probabilistic fibre tracking methods, which evaluates the performance

of a probabilistic algorithm and compares the different probabilistic algorithms using the statistical framework. A thorough quantitative performance analysis is performed on phantom data, including a comparison of two types of average curves for the three probabilistic tracking methods; plus FACT deterministic tracking, using two distance measures between the results and the known true tract, from multiple seed points.

Anatomical variance has proved a useful measure to analyze variability of a population of fibre tracking curves. These dispersion measures help to quantify the geometric extent of each branch and show promise for future clinical application to neurological disorders. We therefore define and estimate second order statistics of the probabilistic curve-set using the statistical framework. The estimation is based on local spatial positions of curves. These measures not only provide descriptive measures of variability but also allow us to generate new data according to the estimated variability, or to compare different probabilistic tracking algorithms on the basis of variability.

2. Statistical framework

2.1. Probabilistic population model

2.1.1. Original curves

The results of probabilistic fibre tracking algorithms, a set of probabilistic tracking curves, are open curves which most likely represent elements of fibre bundles. We define a statistical framework for representing, averaging and measuring second order statistic probabilistic fibre tracking curves in three dimensional Euclidean space $\Re^3$.

Let Γ be a set of N probabilistic fibre tracking curves from a seed point s, where each curve γ_i is defined by a set of k_i ordered points in $m = 3$ dimensions, represented by a $k_i \times m$ matrix.

$$\Gamma = \{\gamma_i, 1 \leqslant i \leqslant N, \gamma_i \in M_{k_i,m}\} \tag{1}$$

Here $M_{n,m}$ denotes the set of all $n \times m$ matrices. Typically N varies between 100 and 10,000 in practice.

2.1.2. Reparameterisation

A problem with these tracking curves γ_i is that uniform steps in the parameter do not correspond to uniform path distances. It is therefore necessary to reparameterise the space curves by arc-length. This allows the look up of a parameter value that corresponds to a desired arc-length. We therefore use an arc-length reparameterisation method, which reparameterises the curves by placing a high number of points at equal arc-length steps on each curve γ_i.

Analytically, a smooth space parametric curve is represented by a mapping $\gamma : I \to \Re^3$ of an interval $I \subset R$ into three dimensional Euclidean space $\Re^3$. Equivalently, the parameterised tracking curve $\gamma(t)$ can be considered a 3-vector of functions:

$$\gamma(t) = \begin{pmatrix} x(t) \\ y(t) \\ z(t) \end{pmatrix}, \quad t \in I \tag{2}$$

In the parameterised curve $\gamma(t)$, parameter t represents the index of the sequence of points and the curve $\gamma(t)$ represents the fibre tract trajectory in 3D space.

2.1.3. Population model

We model the parametric fibre tracking curve-set as an independent realisation of a stochastic process $\Gamma(t)$ that has mean $E\{\Gamma(t)\} = \mu(t)$ and variance $var\{\Gamma(t)\} = \sigma^2(t)$. A random curve from the population may then be expressed as

$$\Gamma(t) = \mu(t) + \epsilon(t) \tag{3}$$

where $\epsilon(t)$ are independent and $E\{\epsilon(t)\} = 0$.

For statistical analysis, we assume a collection of n probabilistic fibre tracking curves, Γ, each curve γ_i is parameterised at points t_1, $t_2, \ldots, t_{mp(i)}$, where $mp(i)$ is the maximum number of points of curve γ_i. The jth point on the ith curve will be denoted by $\gamma_i(t_j)$. The first points on the curves (t_1) are seed points, which are same for all curves γ_i in Γ. The length of the space curve between points $\gamma(t_{k+1})$ and $\gamma(t_k)$ is given by $len = \|\gamma(t_{k+1}) - \gamma(t_k)\|$ where len is the same for all curves γ_i and all pairs t_k and t_{k+1}. In our implementation, we use a constant arc-length step len based on the average arc-length of the set of curves in the collection Γ to reparameterise the curves.

2.2. Distances between curves

The solution of statistical problems by a decision rule based on the notion of distance is a well-known methodology. Two pairwise distances d between curves γ_i and γ_j were implemented here:

2.2.1. The Hausdorff distance

$$d_H(\gamma_i, \gamma_j) = max(d_{H'}(\gamma_i, \gamma_j), d_{H'}(\gamma_j, \gamma_i)) \tag{4}$$

where $d_{H'}$ is the asymmetric Hausdorff distance.

$$d_{H'}(\gamma_i, \gamma_j) = max_{x \in \gamma_i} min_{y \in \gamma_j} \|x - y\| \tag{5}$$

$\|\cdot\|$ is the Euclidean norm and ordered pair (γ_i, γ_j) indicates an asymmetric distance from γ_i to γ_j.

2.2.2. The average closest distance

$$d_A(\gamma_i, \gamma_j) = mean(d_{A'}(\gamma_i, \gamma_j), d_{A'}(\gamma_j, \gamma_i)), \tag{6}$$

where $d_{A'}$ is the asymmetric average closest distance.

$$d_{A'}(\gamma_i, \gamma_j) = mean_{x \in \gamma_i} min_{y \in \gamma_j} \|x - y\| \tag{7}$$

These measures are clearly applicable to probabilistic tracking curves, and can be implemented accurately by making comparisons of distances between the points in the sequences which represent the curves.

2.2.3. Distance matrix

We compute the distance between each pair of curves as described and assemble the measures to create a distance matrix D. Given a pair-wise distance d and a fibre γ_i, d is computed between γ_i and γ_j for all γ_j in $\Gamma, j \neq i$. The matrix D is defined which organises the pair-wise distances d between each pair of curves.

$$DistanceMatrix \quad D = (d_{ij}), \quad i, j = 1, \ldots, n. \tag{8}$$

The matrix D is a real positive symmetric matrix with zeros along the diagonal.

2.3. Average curves

We consider a representative curve from a given collection of curves in space as the average curve of the collection. This paper explores a few of the many possible definitions of average curves, and the situations in which they might be relevant. Clearly the representative curve needs to be as close as possible to all the curves in the collection. This can be achieved by ensuring that the average curve is that which minimises the distance from all the other curves. Two types of average measures are implemented for this work.

2.3.1. Mean curve

For non-parametric estimation of the overall mean curve $\mu(t)$, we use the least squares estimate of μ, which is obtained by averaging the data values separately at each parameter value t.

$$\hat{\mu}(t) = \frac{1}{p(t)} \sum_{i=1}^{p(t)} \gamma_i(t) \tag{9}$$

where $p(t)$ is the number of curves involved in the calculation at t. The mean curve $\hat{\mu}(t) = \gamma_{mean}$ is the centroid of the underlying probability distribution of the probabilistic tracking method.

2.3.2. Median curve

The median curve is selected from the collection as the curve which differs least from all other curves. It is better described as a median, because in the scalar case, there is an interval of real numbers rather than a collection of curves, the one with least maximum variation from the others is midway between the maximum and the minimum.

It may not always be necessary to construct a new average curve to represent the set. If there are a large number of curves it may be possible to select the curve which differs least from the other curves.

In our implementation, we first compute the distance matrix D quantifying similarities between pairs of tracts. We then use the matrix D to identify the best curve(s) from the set of likely curves in the set Γ. We use a hierarchical algorithm to find the median curve(s). The steps below outline the procedure for generating the median curve of a curve-set using a distance measure d.

Step 1: Select the maximum value in the matrix D and find the correspondent curves γ_{C1} and γ_{C2}.

Step 2: Remove the two curves γ_{C1} and γ_{C2} from the set and reorganise the matrix.

Step 3: Repeat steps 1 and 2 for every remaining curve-set and successively remove the curves into a hierarchy of smaller and smaller numbers of curves until one or two curves remain in the set.

Step 4: If the number of resultant curves is two, the mean curve approach described above is applied to the resultant curves in order to produce a single median curve, else the one remaining curve is selected.

2.4. Dispersion measures

Generally a measure of dispersion, the variance $\sigma^2(t)$ of the parametric curve-set $\Gamma(t)$ is defined as:

$$\sigma^2(t) = \frac{1}{n} \sum_{i=1}^{n} \|\gamma_i(t) - \hat{\mu}(t)\|^2 \tag{10}$$

where $\sigma(t)$ provides the local standard deviation values of the curve-set $\Gamma(t)$ at each parameter value t. Globally, we define the standard deviation $STD(\Gamma)$ as a single value of a probabilistic fibre tracking curve-set Γ using different distance measures d as

$$STD(\Gamma) = \sqrt{\frac{1}{n} \sum_{i=1}^{n} d(\gamma_{mean}, \gamma_i)^2} \tag{11}$$

where γ_{mean} is the mean curve of the curve-set Γ and $d(\gamma_i, \gamma_j)$ is a distance measure between curves γ_i and γ_j.

3. Fibre tractography algorithm

3.1. Algorithm

The concept of our algorithm is illustrated by Fig. 1 which shows the output of each stage of the algorithm. We first apply a probabilistic algorithm to generate a number of tracts from a seed point; these tracts, considered as curves, are divided into two groups, forward and backward from the seed point; each of the two sets of curves are then separated further using a clustering algorithm to find all the branch sets. Curves that are very short or long compared to the average arc-length of curves of each branch and curve branches with small number of tracts are excluded from the set. Finally, the average curve methods were applied for each set of branched curves from the seed point and the resultant curves

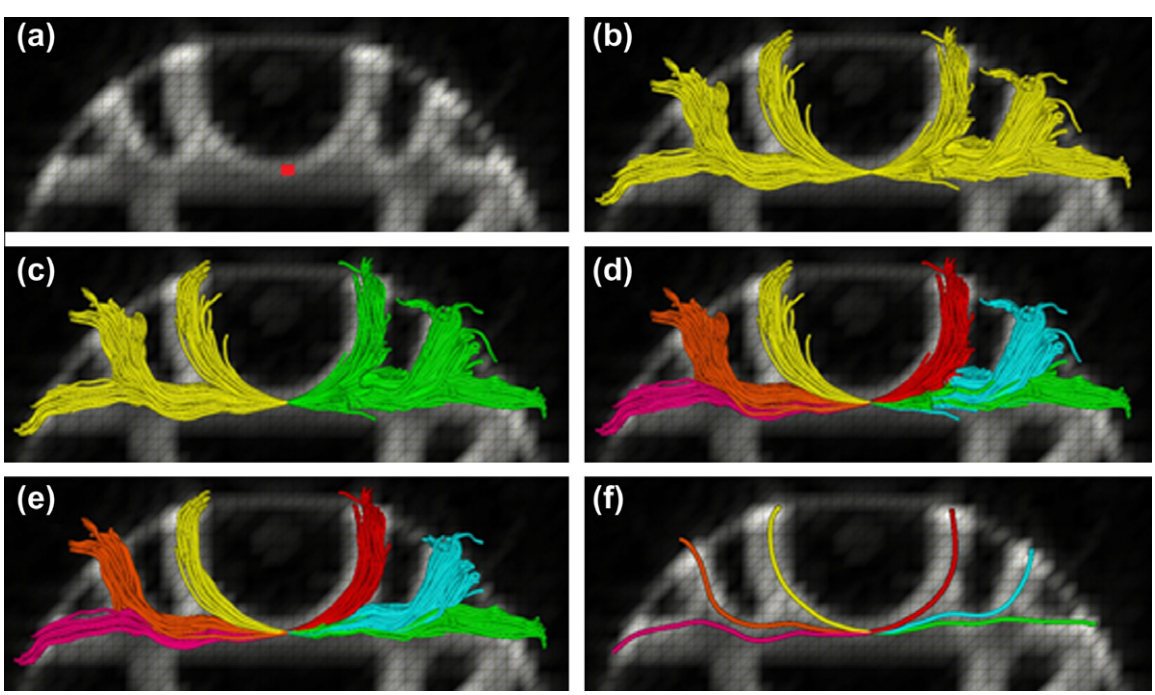

Fig. 1. The six stages of our improved tractography algorithm illustrated using images of a physical diffusion tensor tractography phantom: (a) seed point, (b) probabilistic tracking from the seed point, (c) forward and backward tracts, (d) clustered branches, (e) branches after pre-processing and (f) average curves.

concatenated. The tractography algorithm describing these steps is given by Algorithm 1.

Algorithm 1. The improved tractography algorithm.

Input: A DTI volume, a probabilistic method, a seed point region (ROI) and predefined parameters: l for branching and r, t, c for pre-processing.

Output: Set $\{\gamma_{s_1}, \gamma_{s_2}, \ldots, \gamma_{s_{reg}}\}$, where each γ_{s_k} is a concatenated well defined single curve for all the possible connections from the seed point s_k and reg is the total number of seed points in the ROI.

Repeat

1. **Probabilistic Tracking**: Using a given probabilistic tracking method, generate N tracts as a set of curves Γ from a seed point s.
2. **Forward and Backward Tracts**: Divide the curves Γ based on their direction into forward and backward from the seed point, starting with the primary vector sign:

$$\Gamma_1 = \left\{\gamma_i^1, 1 \leqslant i \leqslant N, \gamma_i^1 \in M_{k_i^1,m}\right\} \text{ and}$$
$$\Gamma_2 = \left\{\gamma_i^2, 1 \leqslant i \leqslant N, \gamma_i^2 \in M_{k_i^2,m}\right\},$$

where $k_i = k_i^1 + k_i^2 - 1$.

3. **Estimate Branches**: Define the branch sets $\Gamma_{1,p}$, $p = 1 \cdots P$ and $\Gamma_{2,q}$, $q = 1 \cdots Q$ for Γ_1 and Γ_2, using the clustering algorithm for estimating branches described below (threshold l), where P and Q are the number of branches.

$$\Gamma_{1,p} = \left\{\gamma_i^{1,p}, 1 \leqslant i \leqslant N_{1,p}, \gamma_i^{1,p} \in M_{k_i^{1,p},m}\right\}, \quad \sum N_{1,p} = N$$
$$\Gamma_{2,q} = \left\{\gamma_i^{2,q}, 1 \leqslant i \leqslant N_{2,q}, \gamma_i^{2,q} \in M_{k_i^{2,q},m}\right\}, \quad \sum N_{2,q} = N.$$

4. **Pre-processing** (**Outlier Removal**): Delete branch set if number of curves in branch < r% of N (very low cardinality) and delete curves in every branch set if the arc-length of the curve < t % or > c% of the average arc-length of the curves (very short curves and very long curves) in the branch.

$$\text{Output}: \ \Gamma_b = \left\{\gamma_i^b, 1 \leqslant i \leqslant N_b, \gamma_i^b \in M_{k_i^b,m}\right\},$$
$$b = 1, \ldots, B \quad \text{where } \sum N_b \leqslant N \text{ and}$$
$$B \leqslant P + Q.$$

5. **Average Curves**: Estimate the average curve γ_{avg}^b for each branch set Γ_b using an average curve algorithm as described above.
6. **Output from the Seed Point**: Concatenate each resulting average curve γ_{avg}^b giving output γ_s from the seed point s.

Until all the seed points from the ROI have been processed.

3.2. Estimation of branching curves

Probabilistic tractography curves result in a set of streamline curves connecting a seed point to distinct anatomical regions. Before the estimation of branches, we separate every curve into two curves based on the seed point (forward and backward) and therefore the whole set of curves are divided into two sets of curves, which share the same starting point (the seed point). We developed a distance-based divisive hierarchical clustering scheme that uses the distance matrix D to find all branches in a curve-set, described by the following steps.

Step 1: The clustering algorithm begins with all the curves γ_i in Γ as a single cluster.

Step 2: Compute the distance matrix D for the curve-set.

Step 3: Select the maximum value in the matrix D and find the corresponding curves γ_{C1} and γ_{C2}.

Step 4: Divide the curves γ_i, $i \neq c1$, $c2$, into two clusters, one related to curve γ_{C1} and the other related to curve γ_{C2} using a measure $\min(d(\gamma_i, \gamma_{C1}), d(\gamma_i, \gamma_{C2}))$.

Step 5: Repeat steps 2, 3 and 4 for every cluster and successively divide the curves into a hierarchy of smaller and smaller clusters until the maximum value of the matrix < l, where l is a threshold to be chosen.

Only one parameter, the threshold l, has to be selected manually. A large value of l results in a small number of branches, whereas a smaller value will result in a larger number of branches. The optimal parameter l depends on the acquisition parameters of the data set and on the choice of the distance metric. The symmetric average closest distance d_A provides a global similarity measure since it integrates closest distances along the whole curve. The symmetric Hausdorff distance d_H is a worst-case distance. It is a useful metric to reject outliers and prevents the algorithm from clustering curves with high dissimilarity.

4. Methods

4.1. Probabilistic tracking method

We investigated the use of three different probabilistic algorithms in this work. The first algorithm was the wild-bootstrap fibre tracking (Jones, 2008) based on the model described in Whitcher et al. (2008). 1000 tensor volumes were generated by fitting the diffusion tensor and a simple 4th order Runge–Kutta streamline method was used to propagate each of the 1000 volumes to generate 1000 tracts from each seed point. The second algorithm was the Bayesian probabilistic tractography algorithm described in Friman et al. (2006). 1000 streamlines were generated from each seed point using the diffusion model, parameter values and likelihood calculations from Friman et al. (2006).

The final algorithm was that of Hagmann et al. (2003) who proposed a random-walk model of a particle diffusing in a DT field D^α to assess uncertainty in tractography described by

$$x_{n+1} = x_n + \mu\Omega_n \tag{12}$$
$$\Omega_n = \lambda d_n + \Omega_{n-1}, (\Omega_n \cdot \Omega_{n-1}) \geqslant 0 \tag{13}$$
$$d_n = D_n^\alpha r_n \tag{14}$$

Here, $\{x_n\}$ are a sequence of points on the fibre path, r_n are random vectors uniformly distributed over a unit sphere, Ω_n is a weighted sum of the random vector d_i, μ is step size and α and λ are parameters of the algorithm. The algorithm was repeated 1000 times from each seed point with $\alpha = 2$ and $\lambda = 1$.

We further considered the performance of our tracking algorithm when two tensors are allowed to cross within a single voxel. The signal attenuation equation for a generalised two-tensor model can be described by a weighted sum of two Gaussian functions Tuch et al. (2002). We used the Levenberg–Marquardt non-linear least squares algorithm to fit a mixture of Gaussian densities to the data. The random-walk algorithms described above are then applied to a two-tensor model to generate probabilistic curves. The probabilistic two-tensor tracking method starts from a given starting position and estimates one trajectory for each of the two tensors. This generates two trajectories per seed point. The random-walk algorithm is then used to propagate the trajectories to the next position. We use the two tensors per position and also the two principal eigenvectors to determine which of the trajectories (if any) should be followed. For each position, we choose the diffusion tensor, which has the 'most similar' principal eigenvector

to the principal eigenvector calculated from the previous position. The most similar eigenvector is the one which has the smallest angular difference. The two-tensor random-walk algorithm was then repeated 1000 times from each seed point.

4.2. Data acquisition

4.2.1. Physical phantom

Diffusion-weighted data were acquired from a physical phantom (Poupon et al., 2008) on a 3T MRI system with $3 \times 3 \times 3$ mm^3 voxel resolution, b value = 1500 s/mm^2 and 65 directions (1 unweighted and 64 diffusion directions). A single-shot diffusion-weighted twice refocused spin echo EPI pulse sequence was used to perform the acquisitions, while compensating for eddy currents to the first order. The acquisition parameters were field of view FOV = 19.2 cm, image size $64 \times 64 \times 3$, repetition time TR = 5 s and echo times TE = 94 ms providing isotropic resolution.

We applied the average curves algorithm to the phantom data, using the three single-tensor probabilistic tracking methods, described above, from 16 pre-defined seed positions with 1000 iterations. In the case of the median curve, we used both symmetric distance measures. The average closest distance was used in the distance matrix D for the clustering algorithm to find all branch sets. The same fibre structures were then extracted using the FACT deterministic algorithm (Mori et al., 1999) using the same parameters (step size = 1 mm and curvature threshold = 60°).

4.2.2. In vivo data

Diffusion weighted images were acquired from a healthy human on a whole-body 1.5 Tesla scanner using a spin-echo EPI pulse sequence with 64 diffusion encoding gradients with a b-value of 1000 s/mm^2 evenly distributed in space and seven images without any diffusion weightings (TE = 100 ms, TR = 12 s, 128×128 image matrix, FOV = 220×220 mm^2). Sixty slices were acquired with 2.4 mm thick interleaved slices (no gap), which covered the whole brain with $2.4 \times 2.4 \times 2.4$ mm^3 spatial resolution.

Random trajectories were initiated from a seed point in the corpus callosum using single-tensor and two-tensor random-walk probabilistic methods and two points in the right/left internal capsule using wild-bootstrapping method with 1000 iterations. The clustering algorithm was applied to the curves using the average closest distance for estimating all of the branch-sets in each seed point. The mean curve method was applied for each set of branched curves from the seed points.

4.3. Quantitative analysis tool

We have developed a suite of tools for quantitative analysis of fibre tracking curves, especially for probabilistic methods. The tools are designed to provide quantitative analysis of fibre curves generated from a tractography algorithm using the curve-based statistics. Here we describe analysis of performance measures of a tracking algorithm and the variability of a probabilistic tracking curve-set.

4.3.1. Performance analysis

Performance measures (ξ) were calculated as the error in tract estimation, which is defined by the distance d between the ground truth curves γ_T of the ideal trajectory and the resultant curves γ_{avg} using the average curve of a probabilistic tracking method from a seed point.

The phantom data was used to test the performance of the deterministic and the average curves of three probabilistic tracking algorithms as the ground truth is known (http://www.lnao.fr/spip.php?article157). The ground truth curves and the average curves of the most probable branches of the probabilistic methods and the FACT method from the 16 seed points of the phantom data were assessed. The two most probable branches from the forward and backward curve-sets were selected from the set of different branches from the seed point as those containing the highest number of curves. The asymmetric average closest distance $d_{A'}$ from γ_s to γ_T, and the asymmetric Hausdorff distance $d_{H'}$ from γ_s to γ_T were used. Mean and standard deviation of ξs are reported for each method.

4.3.2. Statistical analysis

Statistical analysis was carried out using the Minitab-16 statistical package. An upper-tailed student t-test was used to compare the performance measures between the different tracking methods described above. If variance was unequal, the t test used independent variance. The level of statistical significance was set at $p < 0.05$.

4.3.3. Analysis of variability

Here we compare the dispersion measure of the three probabilistic methods curve-sets, which were generated from a range of seed points and propagated in different regions in the phantom data. The standard deviation values *STD* (average *STD* of the forward and backward branches) are calculated from the most probable branches of the three probabilistic methods from the same 16 pre-defined seed points of the phantom data using the symmetric average closest distance (d_A), asymmetric average closest distance ($d_{A'}$), symmetric Hausdorff distance (d_H) and the asymmetric Hausdorff distance ($d_{H'}$). Asymmetric distances were computed from the average curve γ_{avg} to a curve γ_i in the curve-set Γ.

5. Results

5.1. Phantom data

5.1.1. Qualitative results

Fig. 2 shows typical results of our tractography algorithm for each seed point of the phantom data. The mean and median curve resulting from the most probable branches of the Bayesian and wild-bootstrapping algorithms are illustrated in the figure. Only the most probable branch average curves are shown to provide a clearer view. The average curve results are consistent with the ground truth, except where some paths meet crossing regions. A comparison of our tracking method with an implementation of the FACT deterministic method using the same seed points shows that our algorithm is more robust in the presence of complex pathways. The FACT trajectories show unusual tract behaviour, displaying sharp bends and loops, while the average curve trajectories generally do not. The lengths of the resulting FACT tracking curves were also smaller than the average curve lengths, i.e. the average curve pathways propagated further than the FACT tracts. The mean curve tracts are smoother than the median curves and generally show fewer sharp bends in the tracts. These results show how our tractography algorithm is able to give a clear output of fibre bundles from corresponding seed points in a way that is not possible with the output of probabilistic tracking methods. We estimated the computational time for clustering of each seed point. For the clustering experiments considered in Fig. 2, our approach required less than an average of 3 min of processing time (Intel (R) Duo-E4400 CPU and Linux OS).

5.1.2. Performance analysis

Table 1 presents mean and standard deviation values for the performance measures (ξ) in mm for the 16 pre-defined seed points of the phantom data. Mean curves, median curves using symmetric average closest distance (A), and median curves using

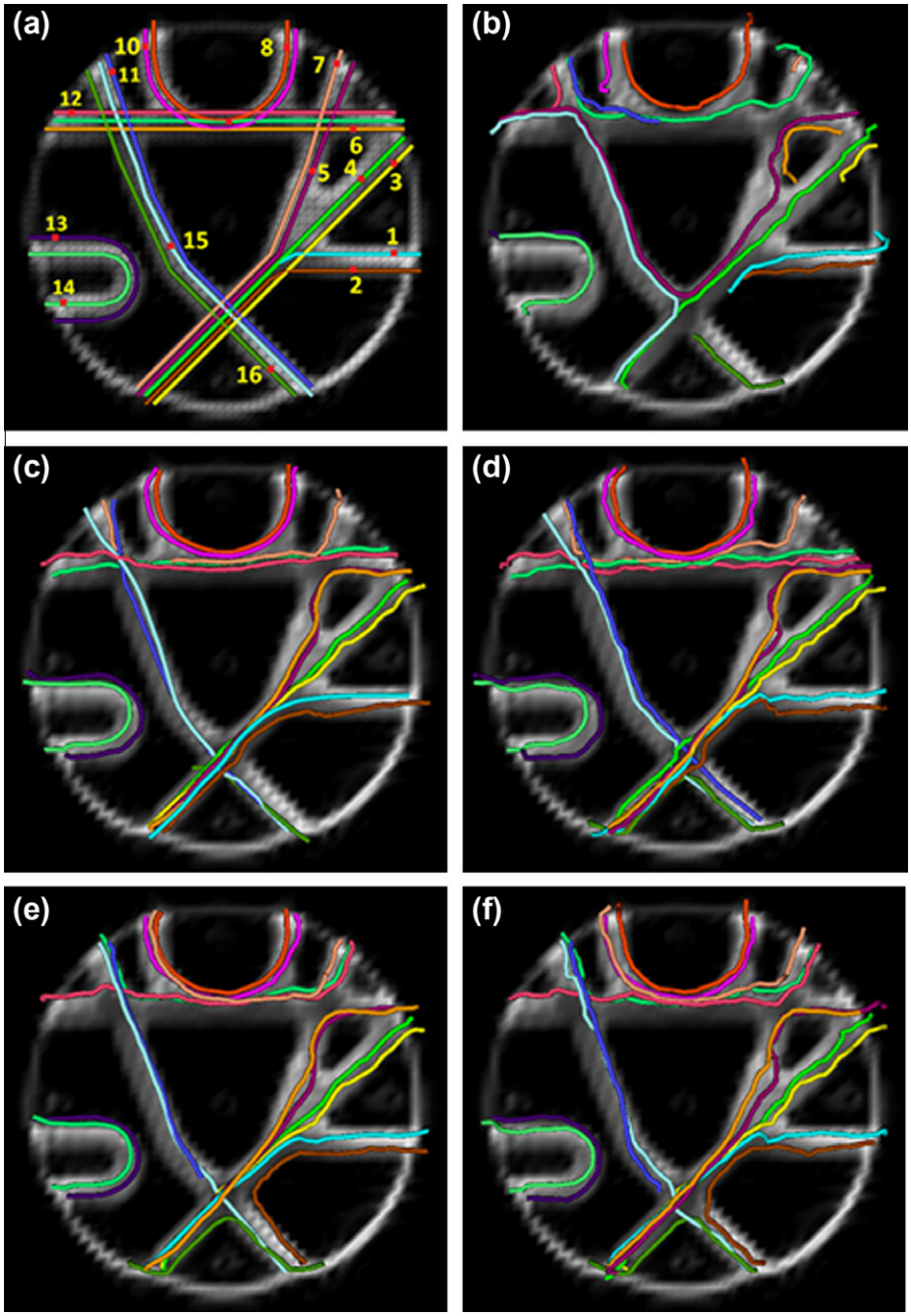

Fig. 2. (a) Ground truth and seed points overlaid on a FA map. Results of (b) FACT, (c) mean and (d) median curves of wild-bootstrapping and (e) mean and (f) median curves of Bayesian tracking.

the symmetric Hausdorff distance (H) of three probabilistic tracking methods and FACT curves are considered to estimate the performance measure ξ.

The statistical analysis results show that the average curve methods are more accurate than the FACT deterministic tracking method with significantly lower errors (FACT vs Wild-bootstrap mean curve with $d_{A'}$, $p = 0.048$). Performance measures of mean curves for the wild-bootstrap, Bayesian and random-walk are not significantly different (Random-walk vs Wild-bootstrap mean curve with $d_{A'}$, $p = 0.269$). However, the individual performance measures of wild-bootstrap results are better than the other two probabilistic methods in all cases. The mean curve results are considerably less than the results of the two distance median curves (Bayesian median curve (d_H) vs Bayesian mean curve with $d_{A'}$, $p = 0.042$) and the median curve results using the symmetric average closest distance are not significantly different from the median curve results using the symmetric Hausdorff distance (Random-walk median curve (d_H) vs Random-walk median curve (d_A) with $d_{A'}$, $p = 0.325$). Here we used asymmetric measures to estimate the error, in order to avoid the accumulation of errors due to early stopping curves or mis-directed paths. Therefore, the distance measurement is calculated using the distance between the resulting curve and the true curve.

5.1.3. Analysis of variability

Fig. 3 shows the comparison of the standard deviation (STD) of the three probabilistic tracking curves using four different distance measures. Considering the scatter plot of standard deviation for the

Table 1
Mean and standard deviation values for the performance measures (ξ) in mm (F – FACT method, W – Wild-bootstrap, B – Bayesian, and R – Random-walk methods).

d	F	Mean curve			Median curve (d_A)			Median curve (d_H)		
		W	B	R	W	B	R	W	B	R
$d_{A'}$	6.25 ± 7.6	2.82 ± 1.3	2.95 ± 1.6	3.18 ± 1.9	3.08 ± 0.8	3.31 ± 1.6	3.67 ± 2.1	3.51 ± 2.1	3.96 ± 1.6	4.08 ± 2.9
$d_{H'}$	17.6 ± 27.8	8.75 ± 8.3	9.74 ± 8.2	11.07 ± 10.1	8.73 ± 7.6	11.04 ± 10.2	13.04 ± 11.4	11.07 ± 11.1	11.08 ± 11.1	14.63 ± 14.1

16 seed points, there is no significant difference between the three tracking methods and it is very difficult to claim that a particular method generates a higher or lower dispersion.

However, generally, the standard deviation increases with the arc-length (or average arc-lengths of a curve-set) of the mean curve and number of curves in the curve-set for all three methods. We observed from Fig. 3 that the curve-sets (initiated from seed points 3, 4, 5, 6, 7, 9, 11, 12, 15 and 16) have larger standard deviations than the short length curve-sets (initiated from seed points 1, 2, 8, 10, 13 and 14) with some exceptions for seed points 11, 16 and 3. Curves originating from seed points 11 and 16 terminate early and the curves from seed point 3 are straight, with little deviation.

For this experiment, we generated the same number of curves (1000) from all seed points using all three probabilistic methods. We used the same threshold l for all the methods and all seed points. However, the number of branches and the number of curves in a branch varied. The random-walk method produced a very high number of branches compared with the other two methods.

In most cases, the number of curves in the most probable branch decreases with the number of well defined branches from the seed point. Generally, standard deviation decreases with seed point and tracking method when the most probable curve-set of the seed point contains low number of curves (not shown in the Fig. 3).

5.2. In vivo data

5.2.1. Corpus callosum

Fig. 4 shows typical results obtained using the single-tensor and two-tensor random-walk methods from a seed point in the splenium of the corpus callosum overlaid on an FA map. The majority of inter-hemispheric pathways are in the corpus callosum, which has the highest anisotropy and moderate curvature. The desired results observed from performing clustering of the corpus callosum are its division into anatomical regions according to the fibre projections. Mean curves of the clusters show representative connections from the seed point to different cortical regions.

Multi-tensor probabilistic tractography can be used to visualise fibre tracts in areas of multidirectional fibre architecture in the brain. Such areas are problematic for single-tensor tractography methods because the single-tensor model cannot describe the complexity of the fibre architecture. Our average curve results of two-tensor deterministic streamline tractography can accurately identify fibre bundles consistent with anatomy, and detect more connected areas than single-tensor streamline tractography. Using more than one seed point will increase the number of branches and

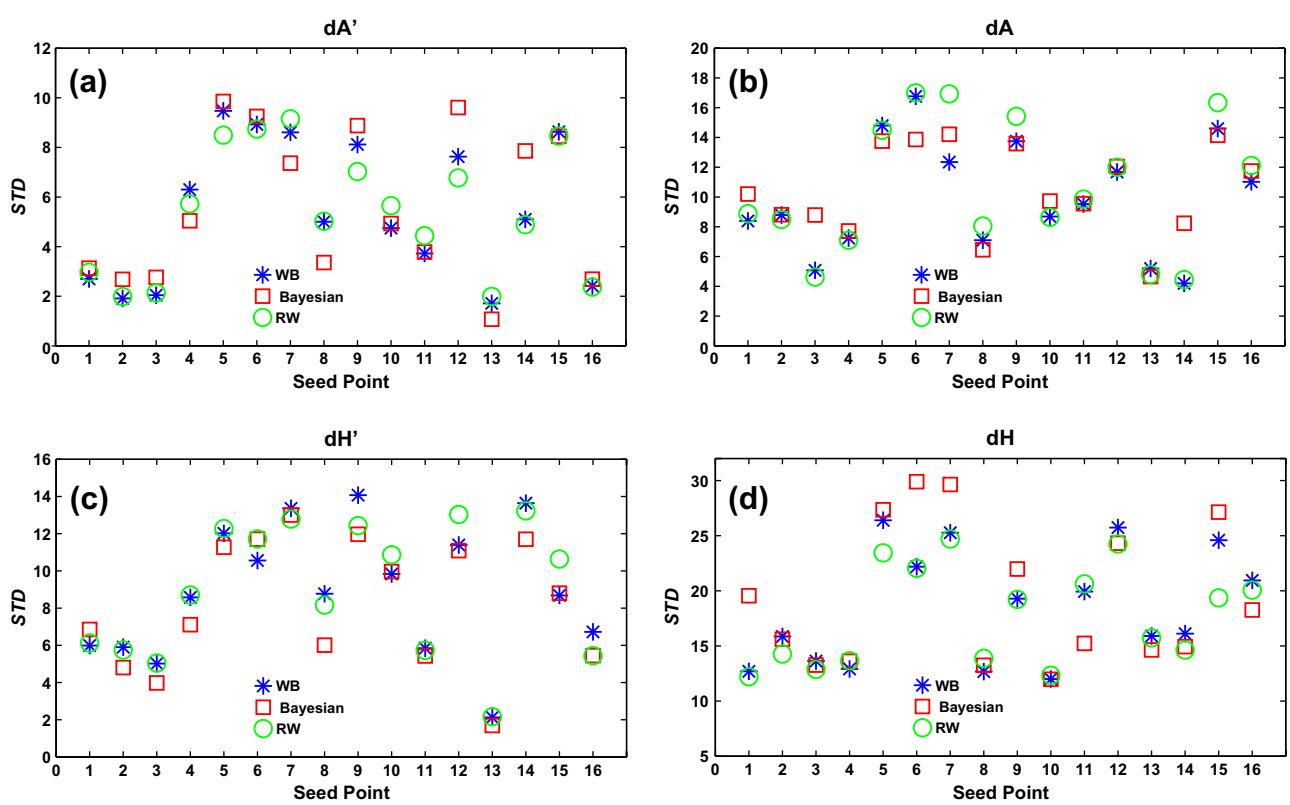

Fig. 3. Comparison of the three probabilistic tracking curves with the standard deviation of the most probable curve-set from 16 seed points using (a) $d_{A'}$, (b) d_A, (c) $d_{H'}$ and (d) d_H distance measures.

average curves. However, we have illustrated the results using a single seed point in order to provide a clear view of the average curves and to simplify the evaluation.

5.2.2. Corticospinal tracts

The corticospinal tracts are a part of the projection fibres system which pass through the internal capsule and form the corona radiata. In order to evaluate the average curves method for probabilistic tracking, the mean algorithm was applied to fibres of the internal capsule, with estimated fibre pathways generated from two seed points using wild-bootstrap tracking. Fig. 5 shows the estimated corticospinal tracts obtained from a seed point placed in the left/right cortico-spinal tract using wild-bootstrap tracking. The generated curves propagate inferiorly through the internal capsule and the results show that our average curves properly reconstruct the fibres to the different motor areas.

Fig. 6 illustrates the combined results of the left and right corticospinal tract from a front view. The clustering results show that the tracts are grouped into different plausible bundles. The output of the wild-bootstrapping method shows that a number of deterministic curves erroneously cross the pons and project into the contralateral hemisphere, while a few trajectories (out of the thousand) crossed the corpus callosum. Fig. 6c shows the mean curves of branches which contain more than 20% of the total number of curves in each forward and backward curve-set and Fig. 6d shows the mean curves of the most probable branches. Anatomically implausible pathways are mostly represented by branches which contain low numbers of curves. When thresholded at >20% of the

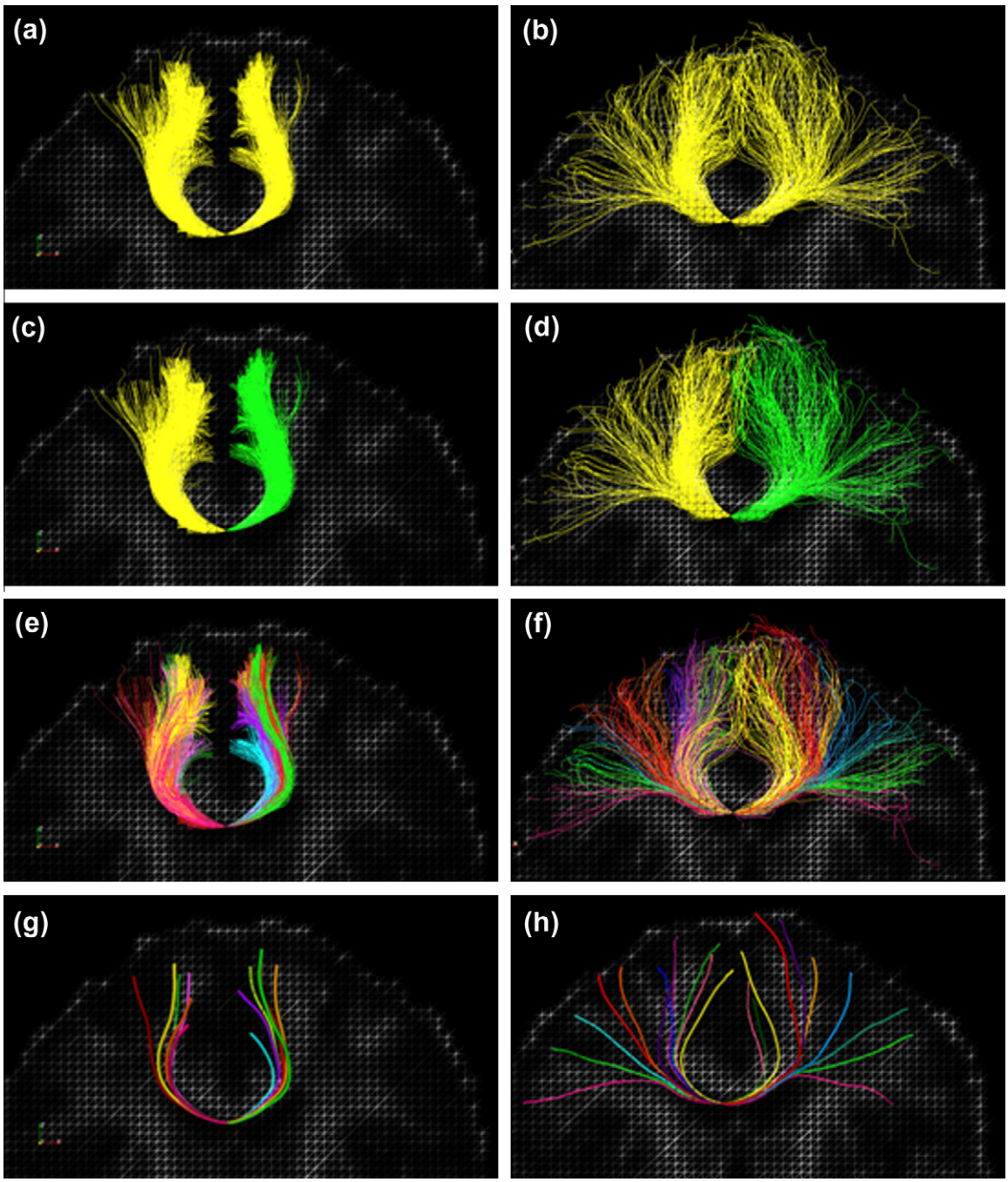

Fig. 4. The results at different stages of improved tractography algorithm using single-tensor (left) and two-tensor (right) random-walk tracking obtained from the seed point placed in the corpus callosum: (a), (b) generated tracts (c), (d) forward and backward tracts (e), (f) clustered tracts and (g), (h) mean curves.

number of curves, the mean curves of the most probable branches show a prominent representation of the most probable path of the probabilistic tracking algorithm.

These examples also show how a framework for average curves of probabilistic tracking is able to handle splitting fibre bundles in a way that is not possible with conventional deterministic tracking.

6. Discussion

DTI tractography is used to investigate important questions about how different anatomical regions of the brain are connected and how these connections alter during development or the progression of disease. Deterministic and probabilistic tractography methods have advantages and disadvantages depending on the algorithm, data, and the underlying diffusion model they use. In this paper, firstly we have described an improved fibre tractography method, which results in a single well-defined trajectory for every strong anatomically distinct connection from a seed point, by taking advantage of both deterministic and probabilistic algorithms using a statistical framework. Secondly, the statistical framework has been used to develop a quantitative analysis tool for probabilistic tracking methods.

The statistical framework described here provides a means of statistically averaging the curves of a probabilistic distribution. An average, central tendency of a data set is a measure of the middle or expected value of the data set in mathematics. The most common method is the mean. The median is an alternative approach to the mean for estimating the average of a set of curves. Dispersion is a key concept in statistical thinking; here we have defined a method to measure the variability of curves from a seed point. The fibre tracts are mostly open curves and the curves are represented numerically as a sequence of points on the curves. Slightly longer or shorter curves should not be regarded as significantly different. The point-sequences are sufficiently dense such that any reasonable interpolant between the points gives essentially the same shape of curve. A natural parameterisation is given by arc-length.

It is often difficult to evaluate the merit of different fibre tracking techniques for reconstructing fibres and the best approach can depend on the application. Deterministic methods are simple and fast and therefore may be used interactively. However, with such approaches, a single error can send the subsequent trajectory off track resulting in an abrupt outcome. Probabilistic methods consider this uncertainty in fibre orientation when calculating estimates of the fibre tracts but it can be extremely difficult to find the most probable path from the output of probabilistic methods. It is also not easy to understand the anatomical connections directly from the connectivity maps. The average curves approaches that we propose here provide not only an estimate of the representation of probabilistic curves but also takes into account an additional measure of uncertainty by considering every possible connection. The results of our tractography approach also shows that the algorithm handles the branching of tracts correctly and the output of the algorithm addresses the challenges associated with the results of traditional probabilistic methods. The average curves have also been shown to be good representations of optimal fibre paths of strong anatomical connections using both phantom and *in vivo* data.

This paper has also presented new techniques for clustering probabilistic curves in 3D, to find anatomically distinct branches and remove outlier curves from a seed point. We found that the use of hierarchical clustering using a fibre similarity measure based on the distance measure between fibres gave the best results. Here, we used four different distance measures between

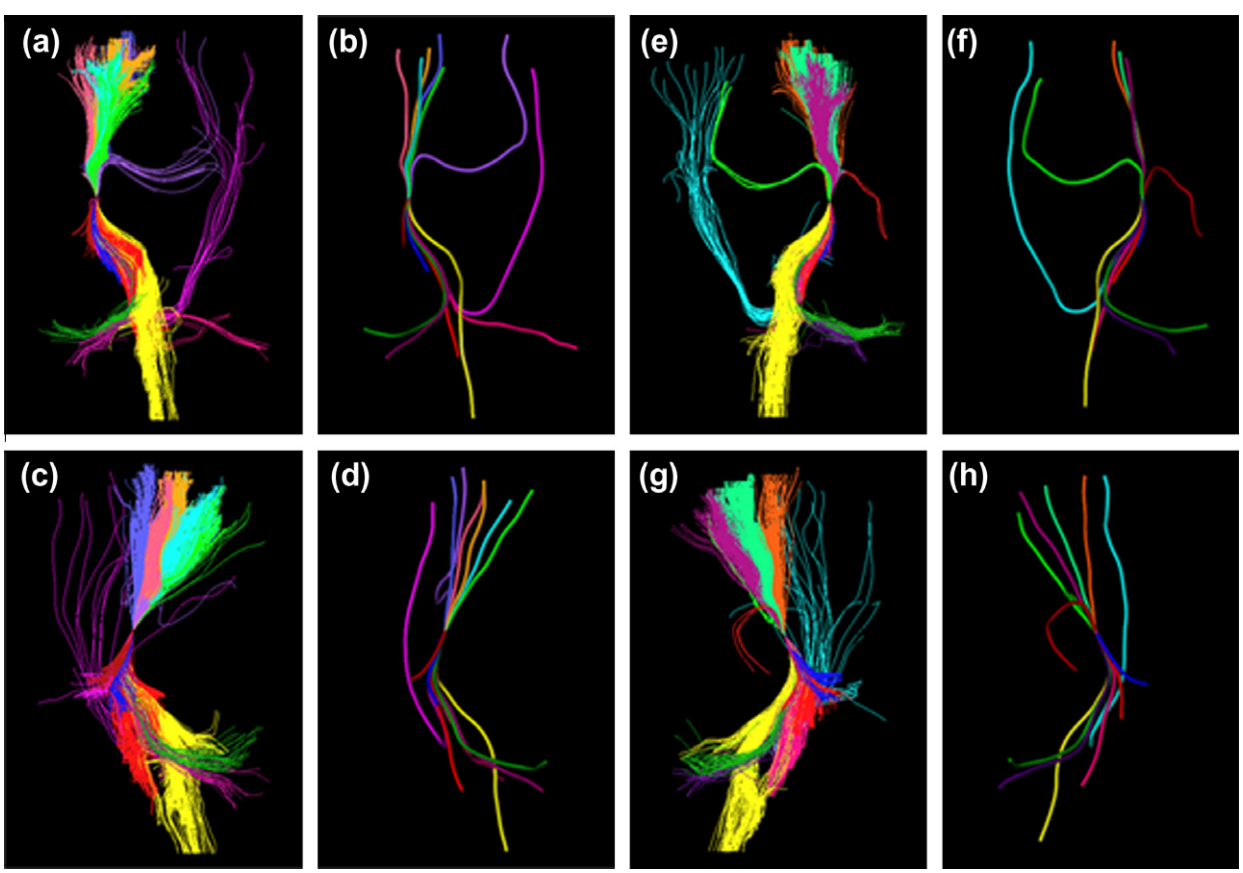

Fig. 5. Improved tractography results using wild-bootstrapping obtained from a seed point placed in the left/right cortico-spinal tract. (a), (c), (e), (g) clustered trajectories and (b), (d), (f), (h) mean curves in front view and lateral view respectively.

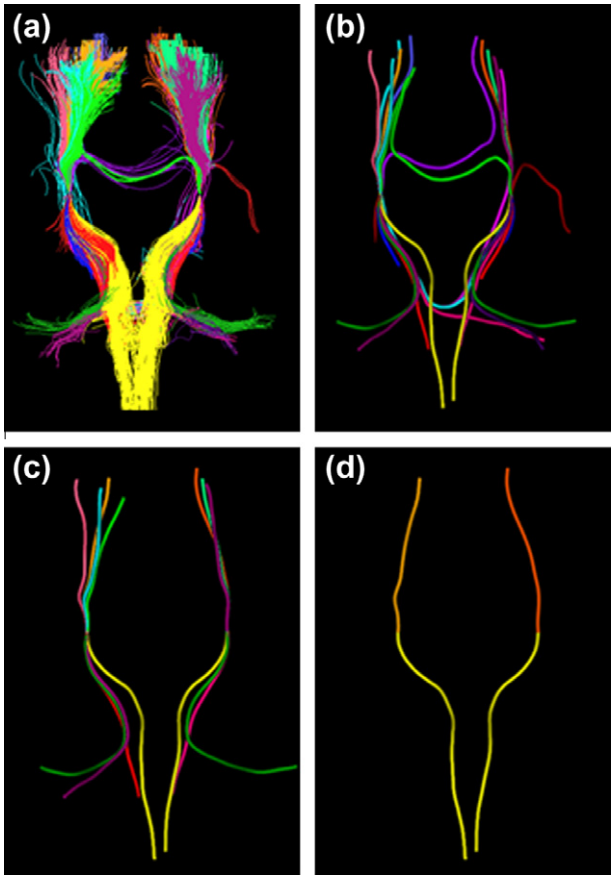

Fig. 6. Improved tractography results using wild-bootstrapping obtained from a seed point placed in the left/right cortico-spinal tract from a front view. (a) Clustered trajectories, (b) mean curves, (c) mean curves of branches which contain more than 20% of the total number of generated curves and (d) mean curve of most probable branches.

curves and we believe these distance measures are a good approximation of the notion of similarity in the domain.

The overall shape of the fibre tract trajectories has been shown to correspond with known anatomy, providing quantitatively useful data. However, there are conceptual and practical issues that must be understood when choosing this approach. The results of our average curves approach depends on the probabilistic methods which we applied. The probabilistic methods still suffer from the general problems of tractography, relying only on the overall shape of trajectories gives an inherent degree of protection against the effects of noise and partial volume. Multi-tensor reconstruction techniques can be used to resolve multiple intra-voxel fibre populations corresponding to known fibre anatomy (Tuch et al., 2002). We have therefore evaluated our tractography algorithm using a two-tensor random-walk method, which accurately identifies fibre bundles consistent with anatomy that were not detected by single-tensor algorithms.

The tractography algorithms that we describe here are fast and relatively easy to implement. The computational cost of this algorithm can vary widely; depending on the resolution of the data set, step size and stopping criteria, seed point and the algorithm parameters supplied by the user. However, generally, the averaging methods are significantly quicker than the time for generating all possible tracts using a probabilistic method from a seed point. Compared with the mean curve method, the median curve method has a higher computational cost. One limitation of our study is that we use some semi-automated parameters to identify the short curves and separate the curves from generated curves. Threshold parameters, step length, seed ROIs, and other parameters could be optimised to provide the most faithful reconstruction of the 'gold standard' average curves.

The choice of 'which type of average is good for a particular problem domain' is heavily dependent on the semantics of the domain. The semantics of the domain may well lead to a description of the curves in terms of their feature structure. If each candidate curve is parsed to give a description in terms of features, then it is possible to average the numerical descriptions/coefficients of those features and then synthesise the curve which has that average description. Therefore, feature-based averaging is a possible option for calculating the average measure, and this is a subject for future work.

Quantitative analysis is a powerful tool for evaluating the performance of fibre tracking algorithms. The accuracy of fibre tractography is influenced by the diffusion tensor measurement's sensitivity to image noise and various other factors. Thus, probabilistic tracking methods may result in deviation from the true fibre tract path and therefore lead to erroneous estimates of connectivity. Several studies (Lazar and Alexander, 2003b; Tournier et al., 2002) have investigated the effects of image noise, tensor anisotropy, step size, and tract geometry on the accuracy of deterministic tractography algorithms. However no error analysis for probabilistic methods has previously been reported in the literature. We have used average curves as a tool to analyse errors from three different probabilistic methods. In this study, a systematic comparison and analysis of variability has been carried out for the curve-sets of three probabilistic methods using different distance measures of standard deviation. The standard deviation increased with the arc-length of the mean curve and number of curves in the curve-set, as expected, but there was no significance difference in the probabilistic algorithms. However, if issues such as bimodality in the probabilistic tracking results are adequately dealt with, such that the average tracts (mean and median) provide a robust result for a given seed point and distance along the tract, then the work presented here could provide a useful method for summarising the quantitative results from such algorithms.

References

Basser, P.J., 1997. New histological and physiological stains derived from diffusion-tensor MR images. Ann. NY Acad. Sci. 820, 123–138.

Basser, P.J., Pajevic, S., Pierpaoli, C., Duda, J., Aldroubi, A., 2000. In vivo fiber tractography using DT-MRI data. Magn. Reson. Med. 44, 625–632.

Batchelor, P.G., Calamante, F., Tournier, J.D., Atkinson, D., Hill, D.L., Connelly, A., 2006. Quantification of the shape of fiber tracts. Magn. Reson. Med. 55, 894–903.

Behrens, T., Woolrich, M., Jenkinson, M., Johansen-Berg, H., Nunes, R., Clare, S., Matthews, P., Brady, J., Smith, S., 2003. Characterization and propagation of uncertainty in diffusion-weighted MR imaging. Magn. Reson. Med. 50, 1077–1088.

Berman, J.I., Chung, S., Mukherjee, P., Hess, C.P., Han, E.T., Henry, R.G., 2008. Probabilistic streamline q-ball tractography using the residual bootstrap. NeuroImage 39, 215–222.

Brun, A., Knutsson, H., Park, H.J., Shenton, M.E., Westin, C.F., 2004. Clustering fiber tracts using normalized cuts. In: Seventh International Conference on Medical Image Computing and Computer-Assisted Intervention (MICCAI'04), Lecture Notes in Computer Science. Rennes – Saint Malo, France, September, pp. 368–375.

Corouge, I., Fletcher, P.T., Joshi, S., Gouttard, S., Gerig, G., 2006. Fiber tract-oriented statistics for quantitative diffusion tensor MRI analysis. Med. Image Anal. 10, 786–798.

Descoteaux, M., Deriche, R., Lenglet, C., 2007. Diffusion tensor sharpening improves white matter tractography. In: SPIE Image Processing: Medical Imaging, San Diego, California, USA.

Descoteaux, M., Deriche, R., Knoesche, T., Anwander, A., 2009. Deterministic and probabilistic tractography based on complex fiber orientation distributions. IEEE Trans. Med. Imag. 28, 269–286.

Ding, Z., Gore, J.C., Anderson, A.W., 2003. Classification and quantification of neuronal fiber pathways using diffusion tensor MRI. Mag. Reson. Med. 49, 716–721.

Durrleman, S., Pennec, X., Trouv, A., Ayache, N., 2009. Statistical models on sets of curves and surfaces based on currents. Med. Image Anal. 13 (5), 793–808.

Friman, O., Farneback, G., Westin, C., 2006. A Bayesian approach for stochastic white matter tractography. IEEE Trans. Med. Imag. 25 (8), 965–978.
Hagmann, P., Thiran, J.P., Jonasson, L., Vandergheynst, P., Clarke, S., Maeder, P., Meuli, R., 2003. DTI mapping of human brain connectivity: statistical fibre tracking and virtual dissection. NeuroImage 19, 545–554.
Jansons, K.M., Alexander, D.C., 2003. Persistent angular structure: new insights from diffusion magnetic resonance imaging data. Inverse Probl. 19, 1031–1046.
Jones, D.K., 2008. Tractography gone wild: probabilistic fibre tracking using the wild bootstrap with diffusion tensor MRI. IEEE Trans. Med. Imag. 27, 1268–1274.
Kreher, B.W., Schneider, J.F., Mader, J., Martin, E., Hennig, J., Il'yasov, K.A., 2005. Multitensor approach for analysis and tracking of complex fiber configurations. Mag. Reson. Med. 54, 1216–1225.
Lazar, M., Weinstein, D., Tsuruda, J., Hasan, K., Arfanakis, K., Meyerand, E., Badie, B., Rowley, H., Haughton, V., Field, A., Witwer, B., Alexander, A., 2003a. White matter tractography using tensor deflection. Hum. Brain Mapp. 18, 306–321.
Lazar, M., Alexander, A.L., 2003b. An error analysis of white matter tractography methods: synthetic diffusion tensor field simulations. NeuroImage 20, 1140–1153.
Lazar, M., Alexander, A., 2005. Bootstrap white matter tractography (BOOT-TRAC). NeuroImage 24, 524–532.
Li, H., Xue, Z., Guo, L., Liu, T., Hunter, J., Wong, S.T., 2010. A hybrid approach to automatic clustering of white matter fibers. NeuroImage 49 (2), 1249–1258.
Maddah, M., Grimson, W.E., Warfield, S.K., Wells, W.M., 2008. A unified framework for clustering and quantitative analysis of white matter fiber tracts. Med. Image Anal. 12, 191–202.
Mori, S., Crain, B., Chacko, V., van Zijl, P., 1999. Three-dimensional tracking of axonal projections in the brain by magnetic resonance imaging. Ann. Neurol. 5, 265–269.
Morris, D., Embleton, K., Parker, G., 2008. Probabilistic fibre tracking: differentiation of connections from chance events. NeuroImage 42, 1329–1339.
O'Donnell, L.J., Kubicki, M., Shenton, M.E., Dreusicke, M.H., Grimson, W.E.L., Westin, C.F., 2006. A method for clustering white matter fiber tracts. AJNR 27, 1032–1036.
Perrin, M., Poupon, C., Cointepas, Y., Rieul, B., Golestani, N., Pallier, C., Riviere, D., Constantinesco, A., Bihan, D.L., Mangin, J.F., 2005. Fiber tracking in q-ball fields using regularized particle trajectories. In: Information Processing in Medical Imaging, pp. 52–63.
Poupon, C., Rieul, B., Kezele, I., Perrin, M., Poupon, F., Mangin, J.F., 2008. New diffusion phantoms dedicated to the study and validation of HARDI models. Magn. Reson. Med. 60, 1276–1283.
Ratnarajah, N., Simmons, A., Hojjat, A., 2009. Stochastic Fibre tracking: an average curves approach. In: Proceedings of the 17th International Society of Magnetic Resonance in Medicine. Honolulu, Hawaii, p. 1436.
Ratnarajah, N., Simmons, A., Hojjat, A., 2010a. A novel average curves tractography technique – validation using a physical phantom. In: Proceedings of the 18th International Society of Magnetic Resonance in Medicine. Stockholm, Sweden, p. 4014.
Ratnarajah, N., Simmons, A., Davydov, O., Hojjat, A., 2010b. A novel white matter fibre tracking algorithm using probabilistic tractography and average curves. Med. Image Comput. Assist. Interv. 13, 666–673.
Savadjiev, P., Campell, J.S.W., Pike, G.B., Siddiqi, K., 2006. 3D curve inference for diffusion MRI regularization and fibre tractography. Med. Image Anal. 10, 799–813.
Tournier, J.D., Alamante, F.C., King, M.D., Gadian, D.G., Connelly, A., 2002. Limitations and requirements of diffusion tensor fiber tracking: an assessment using simulations. Magn. Reson. Med. 47, 701–708.
Tuch, D., Reese, T., Wiegell, M., Makris, N., Belliveau, J., Wedeen, V., 2002. High angular resolution diffusion imaging reveals intravoxel white matter fiber heterogeneity. Magn. Reson. Med. 48 (4), 577–582.
Tuch, D., 2004. Q-ball imaging. Magn. Reson. Med. 52, 1358–1372.
Wassermann, D., Bloy, L., Kanterakis, E., Verma, R., Deriche, R., 2010. Unsupervised white matter fiber clustering and tract probability map generation: applications of a Gaussian process framework for white matter fibers. NeuroImage 51 (1), 228–241.
Wedeen, V.J., Wang, R.P., Schmahmann, J.D., Benner, T., Tseng, W.Y., Dai, G., Pandya, D.N., Hagmann, P., D'Arceuil, H., de Crespigny, A.J., 2008. Diffusion spectrum magnetic resonance imaging (DSI) tractography of crossing fibers. NeuroImage 41, 1267–1277.
Whitcher, B., Tuch, D.S., Wisco, J.J., Sorensen, A.G., Wang, L., 2008. Using the wild bootstrap to quantify uncertainty in diffusion tensor imaging. Hum. Brain Mapp. 29 (3), 346–362.